ORIGINAL PAPER
ΕΡΕΥΝΗΤΙΚΗ ΕΡΓΑΣΙΑ

....

Complete regeneration of the pancreas including islets of Langerhans, acinar cells, centro-acinar cells, intercalated duct cells, and secretory duct cells in Lewis rats

T. Nakatsuji

....

Department of Transfusion Cell Therapy, Hamamatsu University School of Medicine, Hamamatsu, Japan

Πλήρης αναγέννηση του παγκρέατος, περιλαμβανομένων των νησιδίων του Langerhans, των κυττάρων των αδενοκυψελών, των κυττάρων του κέντρου των κυψελών, των διάμεσων και των εκκριτικών κυττάρων των πόρων σε ποντίκια Lewis

Περίληψη στο τέλος του άρθρου

OBJECTIVE Elucidation of *in vivo* systems for complete pancreatic regeneration in animal models. METHOD Using only syngeneic Lewis rats, whole liver, bone marrow (BM) with bone, BM clot, or nonparenchymal liver tissue was transplanted into the host pancreas. In addition, either insulin-like growth factor-1 receptor (IGF-1R) monoclonal antibody (mAb) or vascular endothelial growth factor (VEGF) Ab was injected into the host spleen. The experimental rats were followed for 5.5–6 months. Insulin-like growth factor binding protein 2 (IGFBP2) was examined in hematopoietic mononuclear cells (MNC) and pancreatic cells using flow cytometry (FCM). Electron microscopic analyses were applied for the embryological studies of regenerated pancreas. RESULTS Complete pancreatic regeneration, including both the endocrine and exocrine cells, was confirmed in 2 (50%) of 4 females receiving BM clot grafts and VEGF Ab, in 1 (17%) of 6 males receiving whole liver grafts and IGF-1R mAb, and in 3 (60%) of 5 males receiving nonparenchymal liver grafts and VEGF Ab. On FCM, weakly-positive IGFBP2 cells were increased due to rebound activation of injected IGF-1R mAb. IGFBP2 was also expressed in islet β-cells. Islet progenitor cells smaller than erythrocytes regenerated in blood vessels and developed outside of the vessels. Centro-acinar progenitor cells smaller than erythrocytes regenerated in a microcapillary, the walls of which were destroyed after the full development. Acinar cells proliferated through the mitosis of mature cells outside of blood vessels. CONCLUSIONS Nonparenchymal liver and BM clot grafts produced identical results of pancreatic regeneration. It was concluded that epiblast/germ line-derived host BM cells were mobilized to the grafts, resulting in complete pancreatic regeneration.

Diabetes mellitus (DM) is a progressive disease that is prevalent worldwide. Disturbed insulin biosynthesis in the β-cells of the islets of Langerhans is the cause of DM. β-cell replacement therapy using transplantation is an attractive alternative to insulin injection, because sufficient amounts of insulin are automatically produced *in vivo* when β-cell replacement is successful.

Recently, a new pancreatic stem cell line, which produces insulin from pancreas-related genes, has been established without genetic manipulation.[1] It was reported that pluripotent stem cells, embryonic stem cells (ESC), and induced pluripotent stem cells (iPSC) were a potentially abundant source of both hepatocytes and β-cells.[2] The conversion of liver cells towards a pancreatic endocrine function has been suggested as a possible clinical treatment for DM.[3]

The liver is capable of extensive auto-regeneration through the mitosis of mature cells. Auto-liver grafts can therefore be used for auto-pancreatic β-cell replacement, even in humans. From an embryological view of hematopoietic stem cells, primordial germ cells (PGC) induce the first wave of embryonic hematopoiesis in the aorta-gonad-mesonephros region (AGM), and subsequently, the AGM-hematopoietic stem cells (HSC) form colonies in the fetal liver, thymus, spleen, and during adulthood, in the bone marrow (BM).[4] It has been reported that the stem (epiblast/germ line-derived) cells that subsequently develop into the ectoderm (skin, brain, mammary tissue, etc.), endoderm (gut, liver, pancreas, lung, etc.), and mesoderm (bone, muscle, connective tissues, cartilage, BM, blood cells, vessels, etc.) are deposited in various organs, and persist in these locations into adulthood.

In this study, complete pancreatic regeneration including, both the endocrine and exocrine cells, was achieved by syngeneic Lewis rat transplantation of either a liver graft or a BM clot graft into the host pancreas. Nonparenchymal liver and BM clots showed the ability to develop new pancreatic cells in combination with vascular endothelial growth factor (VDGF) Ab injected into the host spleen, which suggested a new clinical application for β-cell replacement therapy. The histopathology of the regenerated pancreatic tissue, analyzed using a transmission electron microscope, and the flow cytometry (FCM) findings for insulin-like growth factor binding protein 2 (IGFBP2) are demonstrated to confirm the origin of the cells of complete pancreatic regeneration, and its regenerative processes.

MATERIAL AND METHOD

Animals

Male and female Lewis (LEW/SsN) rats were purchased from Japan SLC Co Ltd (Hamamatsu, Japan) and bred and maintained at the animal center of Hamamatsu University School of Medicine. Lewis rats of the second generation were used as experimental rats at the age of 8 to 9 weeks. All transplantations were performed between syngeneic Lewis rats.

Experimental design

This study was composed of 6 experimental (Exp) groups, A, B, C, D, E, and F. In Exp A, 4 Lewis females had a mean body weight (BW) of 159±2 g at the time of a partial pancreatic resection of a piece of pancreatic tissue weighing 0.27 g. They were followed for 6 months post-pancreatic resection without any further treatment. In Exp B, 4 Lewis female hosts had a mean BW of 165±3 g at the time of the syngeneic donor spleen transplantation. A quarter of the female donor spleen was bound to the donor pancreas weighing 0.15 g to produce a combined graft. The combined graft was then attached to the host spleen and pancreas. Anti-insulin-like growth factor-1 receptor (IGF-1R) antibody (Ab) [purified mouse monoclonal antibody (mAb)] was injected into the host spleen at a concentration of 0.3 µg per rat (Calbiochem, Darmstadt, Germany). The IGF-1R mAb used in this study prevents insulin-like growth factor-1 (IGF-1) from binding to its receptor which has tyrosine kinase activity. The IGF-1R mAb binds weakly to the insulin receptor. The rats were followed for 6 months post-transplantation. In Exp C, 4 Lewis female hosts had a mean BW of 158±6 g at the time of the syngeneic transplantation by BM clots. The female donor BM clots contained more than 10^8 cells including microenviromental cells. The BM clot graft enclosed in the donor pancreatic tissue weighed 0.15 g per rat, and each graft was covered with an oblate bag. The BM clot grafts were transplanted by wrapping them in host pancreatic tissue. VEGF Ab, which has been raised against amino acids 1–140 of human VEGF, is an affinity purified

polyclonal Ab that has reacted to mouse, rat, and human VEGF (Santa Cruz Biotechnology, Inc, Santa Cruz, CA, USA). Anti-VEGF Ab (0.4 µg per rat) was injected into the host spleen. The rats were followed for 5.8 months post-transplantation. In Exp D, 6 Lewis male hosts had a mean BW of 238±4 g at the time of the syngeneic liver transplantation. A piece of the female whole liver weighing 0.18 g was wrapped in donor pancreatic tissue, which weighed 0.1 g, and transplanted into the host pancreas. Anti-IGF-1R mAb (0.3 µg per rat) was injected into the host spleen. The rats were followed for 6 months post-transplantation. In Exp E, 6 Lewis male hosts had a mean BW of 241±13 g at the time of the syngeneic BM transplantation into the host pancreas. Small pieces of male BM containing bone (BM-bone) weighing 0.34 g per rat were wrapped in donor pancreatic tissue (0.1 g per rat) and covered with an oblate bag. The BM-bone grafts were then transplanted into the host pancreas. Anti-IGF-1R mAb (0.3 µg per rat) was injected into the host spleen. The rats were followed for 6 months post-transplantation. In Exp F, 5 Lewis male hosts had a mean BW of 265±9 g at the time of the syngeneic transplantation of the female donor liver. From a whole liver weighing 2.55 g, 0.9 g of hepatocytes were removed, and then a piece of the hepatocyte-depleted liver weighing 0.28 g per rat was grafted into the host pancreas after the graft had been wrapped in donor pancreatic tissue weighing 0.1 g. Anti-VEGF Ab (0.4 µg per rat) was injected into the host spleen. They were followed for 5.5 months post-transplantation.

Pathological findings

For light microscopic analyses, the pancreatic grafts were fixed in 10% formalin (Sigma-Aldrich, St Louis, MO, USA) and stained with hematoxylin-eosin (H-E) for all Exp rats. For transmission electron microscopic (TEM) analyses, two methods were employed. The first was no-treatment fixing, and the second involved immunochemical staining before fixation. The pancreatic grafts of the Exp D-5 and Exp F-3 and 5 rats were fixed in 2% glutaraldehyde for 2 hours without pre-treatment. The host spleens of the Exp D-2 and Exp E-1 rats, the host BM of the Exp D-2 rats, and the host pancreases of the Exp D-1 and 5 rats were pre-treated immunochemically before being fixed in 2% glutaraldehyde for 2 hours, and cell suspensions were made from all of the above. The anti-IGFBP2 Ab was affinity purified goat polyclonal Ab raised against a peptide mapping to the C-terminus of mouse IGFBP2 (Santa Cruz Biotechnology, Inc, Santa Cruz, CA, USA). All cell suspensions except for the spleen cells of the Exp D-1 male, which were stained with IGF-1R mAb (0.4 µg per tube), were stained with anti-IGFBP2 Ab (0.6 µg per tube) for 15 minutes at 4 °C. Among them, only the pancreatic cells were incubated for 10 minutes. After being washed once with phosphate buffered saline (PBS), they were incubated further with sheep anti-mouse mAb raised against mouse IgG_1 (0.1 µg per tube), which was conjugated with 15 nm-gold colloidal particles, for 7 minutes at 4 °C (EY Laboratories, Inc, Santa Mateo, CA, USA). After being washed once with PBS, all the cells stained with gold particles were fixed in 2% glutaraldehyde and post-fixed with 1% osmium tetroxide. The sections were doubly stained with uranyl

acetate-lead citrate in order to produce electron micrographs. Light micrographs were taken using a BX51 light microscope containing a DP72 digital camera (OLYMPUS, Tokyo, Japan). Transmission electron micrographs were taken using a JEM 1200 TEM (JEOL, Tokyo, Japan).

Flow cytometry (FCM) analyses

One million cells were sampled from the BM and spleen of all the Exp rats at the time of sacrifice. Additionally, one million cells were sampled from the BM graft of the Exp E-5 males, the spleen grafts of the Exp B-1 and 3 females, and the host pancreases of the 4 Exp A females. They were assessed using an EPICSR XL-MCL system III FCM (Beckman Coulter, Fullerton, CA, USA). Only mononuclear cells (MNC) were selected in the FCM counting. The BM cells were stained with anti-R-phycoerythrin (R-PE)-conjugated mouse anti-rat CD90 (Thy-1)/mouse CD90.1 (Thy-1.1) mAb, which was raised against the rat thymocyte Thy-1 antigen (BD Biosciences, Tokyo, Japan), and anti-IGFBP2 Ab. The pancreatic cells were stained with anti-IGFBP2 Ab and anti-insulin/proinsulin (rat) mAb (Biogenesis Inc, Kingston, NH, USA). The spleen cells were stained with anti-rat CD8a mAb labeled with fluorescein isothiocyanate (FITC) (Cedarlane Laboratories Ltd, Hornby, Ontario, Canada), anti-rat CD25 mAb, that was interleukin 2 receptor (IL-2R) mAb, labeled with FITC (Cedarlane Laboratories Ltd), IGFBP2 Ab, and IGF-1R mAb. Anti-rat CD8a mAb recognizes the majority of natural killer (NK) cells and a subset of peripheral T cells. Anti-rat CD25 mAb recognizes activated T cells and thymic dendritic cells. The concentration of the labeling Ab in each tube was as follows: Thy-1 mAb: 0.4 µg, IGFBP2 Ab: 0.6 µg, insulin mAb: 2.4 µg, CD8a mAb: 0.7 µg, CD25 mAb: 0.1 µg, and IGF-1R mAb: 0.3 µg. One million cells were incubated with each Ab for 30 minutes at 4 °C. The non-fluorescein IGFBP2 Ab, insulin mAb, and IGF-1R mAb that bound to their antigens were incubated further with FITC conjugated monoclonal mouse IgG$_1$ (0.4 µg per tube) (Ancell Co, Bayport, MH, USA) for 15 minutes at 4 °C. The strongly-positive IGFBP2 cells were separated from the weakly-positive IGFBP2 cells based on their peaks, as shown in figures 4a and 4b. The percentage of the weakly-positive IGFBP2 cells was calculated by deducting the strongly-positive IGFBP2 cell percentage from the sum percentage of the weakly- and strongly-positive cells.

As sexual dimorphism was detected in the expression pattern of IGFBP2, the FCM results of IGFBP2 were separated into male and female. As the positive peak of IGF-1R was not separated from the negative peak, the positivity threshold was chosen based on the data for the control males, as shown in figure 4b. The control males were assumed to have a main negative peak.

RESULTS

Complete pancreatic regeneration, including the islets of Langerhans, acinar cells, and duct cells, was attempted using 6 Exp groups (A, B, C, D, E, and F). In Exp groups C, D, and F, but not Exp group E, complete pancreatic regeneration was achieved. The Exp A females, which underwent partial pancreatic removal, did not achieve complete regeneration. The 4 Exp A females, which had a mean BW of 253±10 g, showed a mean pancreatic weight (PW) of 0.33±0.02 g at the time of sacrifice, 6 months after 0.27 g of each of their pancreases had been removed. The four control females (CF), which had a mean BW of 256±10 g, demonstrated a mean PW of 0.51±0.01 g. Therefore, during the 6 month study period, a mean increase in PW of about 0.1 g was calculated to have occurred in the Exp A females. Enlarged lymph nodes (LN), apoptotic islet cell masses in which hemosiderin was deposited, and localized lymphocyte infiltration containing many giant cells were observed at the dissection sites in the Exp A females. Exp B was not designed to examine complete pancreatic regeneration. Instead, it was designed to determine the effects of anti-IGF-1R mAb on syngeneic immune reactions. The Exp B females showed marked intra-pancreatic LN enlargement. In the medullary sinuses of the LN, many auto-erythrocytes bound to sensitized macrophages to form rosettes, and hemosiderin deposits were observed in the rosette-forming macrophages.

Table 1 summarizes the histopathologically confirmed data concerning complete pancreatic regeneration triggered by syngeneic liver grafts and BM grafts. In the 4

Table 1. Histopathological confirmation of complete pancreatic regeneration developed in syngeneic liver and bone marrow (BM) grafts (figures 1a and 1b).

Exp No (Sex)	Total rats (n)*	Kinds of graft	Spleen injection	Complete regeneration	
				- Rat no	(n) (%)
C (F)	4	BM clot	VEGF Ab	- 1, 3	2 (50)
D (M)	6	Whole liver	IGF-1R mAb	- 4	1 (17)
E (M)	6	BM with bone	IGF-1R mAb	None	0 (0)
F (M)	5	Modified liver**	VEGF Ab	- 2, 3, 5	3 (60)

* Number, ** Hepatocytes were removed from the whole liver

BM: Bone marrow, VEGF Ab: Anti-vascular endothelial growth factor antibody, IGF-1R mAb: Anti-insulin-like growth factor-1 monoclonal antibody

Exp C females, which had BM clots grafted into their pancreas and were treated with VEGF Ab, only the Exp C-4 rat discharged pus from its BM clot graft at 20 days post-transplantation. Exp C-1 and 3 female rats (50% of Exp C) showed the same complete pancreatic regeneration as shown in figures 1a and 1b. However, in their acinar cell masses, secretory ducts were regenerated more abundantly, suggesting that the regenerated acinar cells were spread more diffusely in these masses. Secretory ducts were regenerated more actively than acinar cells in the BM clot grafts. Regenerated islets of Langerhans were detected in the masses, as well as elsewhere. Small masses composed of 2–3 acinar cells were often observed in the BM clot grafts. The hematopoietic microenviromental cells that surrounded blood vessels were shown to be very important for complete pancreatic regeneration, because BM-bone grafts did not develop complete pancreatic regeneration, as stated below in more detail. Mildly ischemic changes without vascular regeneration played an important role in complete pancreatic regeneration during the 5.8 month post-transplantation follow-up period. Among the 6 Exp D males, in which a piece of syngeneic whole liver was transplanted into their pancreas in combination with IGF-1R mAb treatment, the Exp D-3 rat discharged pus 30 days post-transplantation. The Exp D-4 male (17% of the Exp D males) achieved complete pancreatic regeneration 6 months post-transplantation, but the grafts of the

other 5 Exp D rats showed necrosis or marked apoptotic atrophy. As shown in figure 1a, the Exp D-4 rat generated new pancreas from a syngeneic donor liver. Small masses of newly generated acinar cells, which stained darkly with H-E, were observed together with islets of Langerhans and secretory ducts after donor hepatocytes fell into apoptosis. Among the 6 Exp E males that received BM-bone grafts and IGF-1R mAb treatment, the Exp E-4 rat discharged pus from its BM-bone graft 28 days post-transplantation. Some BM-bone grafts in the host pancreas were in good conditions at 6 months post-transplantation, when the BM cells were completely surrounded by bone. But, the BM-bone grafts with bone-free spaces became hypoplastic. The Exp E-5 and 6 rats showed necrotic changes in their BM-bone grafts at the time of sacrifice. The Exp E-6 rat, which displayed extensive BM-bone graft necrosis, demonstrated apoptotic islet cell proliferation in its vessels, which had stayed in a relatively good condition. Some BM cells migrated from the BM-bone grafts and demonstrated the ability to develop into islet cells in host pancreatic venous vessels. Around the BM-bone grafts, an area of secretory duct proliferation, acinar cell loss, and development of islets of Langerhans was observed. Complete pancreatic regeneration was not achieved in any of the Exp E males, which received BM-bone grafts. Among the 5 Exp F males, none of them discharged pus from their nonparenchymal liver grafts, which were made from a whole liver with its hepatocytes
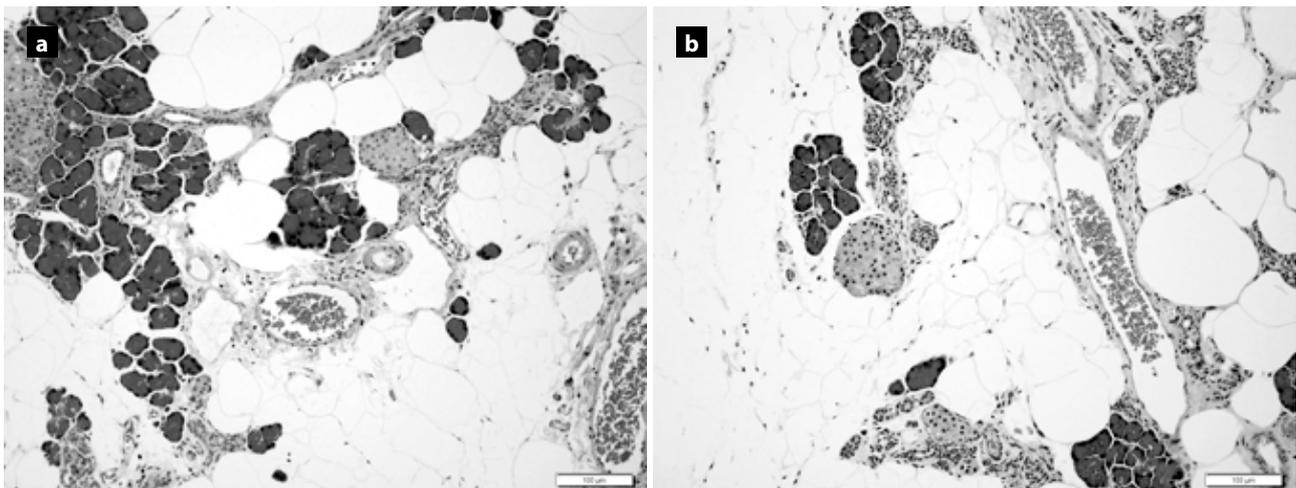

Figure 1. (a) Light micrograph (H-E stain, ×200), showing complete pancreatic regeneration achieved in the Exp D-4 male. The whole liver graft had been transplanted in combination with IGF-1R mAb 6 months previously. The nonparenchymal liver structure remained, but no normal hepatocytes were detected. Many acinar cell masses, which were stained darkly with H-E, had been regenerated in the sinusoidal spaces and portal areas. In the upper-left corner, large islets of Langerhans can be observed, and small islets of Langerhans are present toward top center of the figure. Secretory ducts are present near the acinar cell masses. However, only single acinar cells without any ducts are observed. The scale bar indicates 100 μm. (b) Light micrograph (H-E stain, ×200) showing complete pancreatic regeneration achieved in the Exp F-2 male, into which a piece of nonparenchymal liver had been transplanted in combination with VEGF Ab treatment 5.5 months previously. Small acinar cell masses and islets of Langerhans were observed, as seen in figure 1a. Secretory ducts were generated more actively in these masses than in those shown in figure 1a. The scale bar indicates 100 μm.

removed. The Exp F males were injected with VEGF Ab at the time of the transplantation. The Exp F-2, 3, and 5 males (60%) showed complete pancreatic regeneration. Figure 1b shows complete pancreatic regeneration observed in the Exp F-2 male. Newly generated acinar cells, secretory ducts, and islets of Langerhans were observed, as in the Exp D-4 male (fig. 1a), but more abundant secretory duct regeneration was observed on the exterior of the acinar cell masses than in those of the Exp D-4 male. The Exp F group showed the best complete pancreatic regeneration results among the 4 groups listed in table 1. However, basically identical results were obtained from the BM clot graft and liver graft experiments.

Figure 2a shows a TEM of the newly generated islets of Langerhans found in the Exp F-3 male. In a blood vessel, islet progenitor cells smaller than erythrocytes were newly generated, and the movement of small islet cells from the vascular interior to the vascular exterior was confirmed. Around the vessel, immature β cells developed into mature cells. Among the islet cells, an α-cell was detected. It was confirmed that the newly formed islet cells were capable of normal secretion of insulin and probably also of glucagon, gastrin, and somatostatin, although no δ-cells were shown.

Immature small islet cells were mobilized in the blood vessels, resulting in the proliferation of mature large islet cells around the outside of the vessels. After the islets of Langerhans developed completely, the vessels containing small regenerative cells were suspected to be destroyed by apoptotic changes. Figure 2b shows the same regenerated pancreas as figure 2a. Zymogen granules from acinar cells were secreted into an intercalated duct. Newly generated acinar cells with narrow cytoplasm and a large nucleus demonstrated a very well-developed granular endoplasmic reticulum (GER) and no zymogen granules. Figures 3a and 3b are electron micrographs of newly generated pancreatic cells that were found in the Exp F-5 male. In a microcapillary, a centro-acinar progenitor cell that was very immature and smaller than an erythrocyte had regenerated, and the walls of the microcapillary had been destroyed after the centro-acinar progenitor cell had fully developed. The first acinar progenitor cell to develop, although which was detected by light microscopic analysis, could not be shown on electron micrographs. It was confirmed that acinar cells proliferated through the mitosis of mature acinar cells outside of blood vessels. In the graft sections of the Exp D-5 rat, no pancreatic regeneration was detected by either
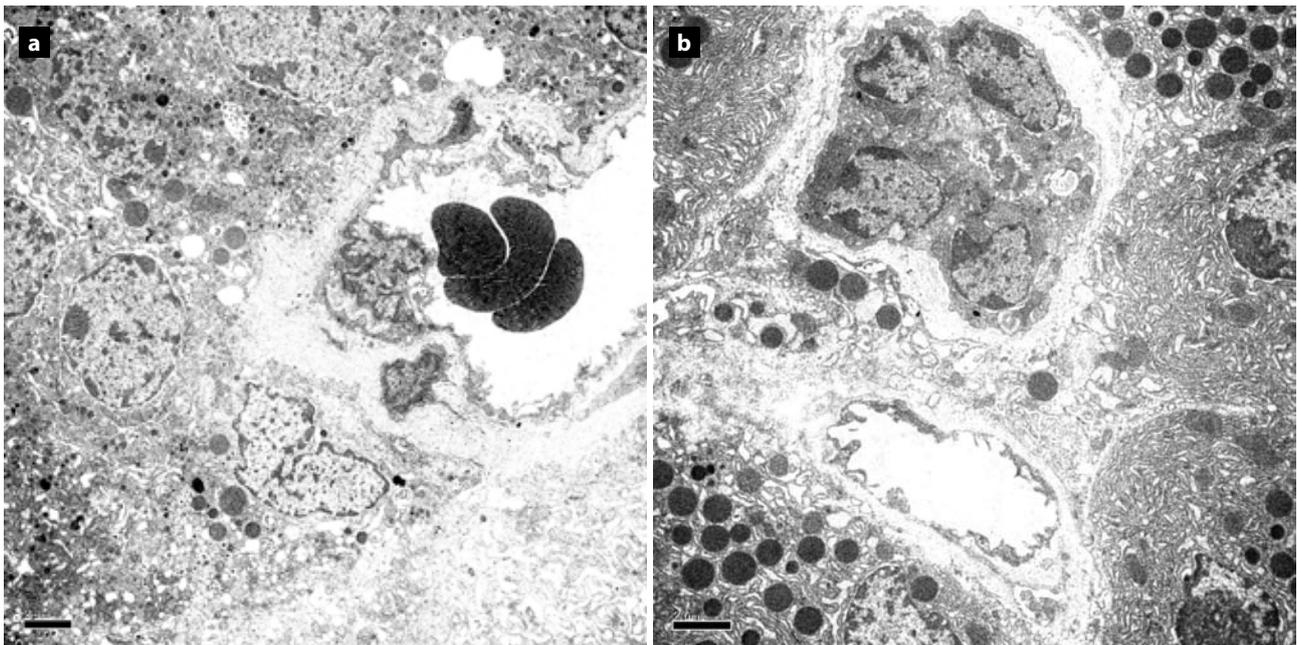

Figure 2. (a) Transmission electron micrograph (Uranyl acetate-lead citrate stain, ×5,000) of nonparenchymal liver graft from the Exp F-3 rat (The light microscopic analyses of the Exp F-3 graft showed complete pancreatic regeneration). On the right, a blood vessel containing red blood cells is shown. Two islet progenitor cells that are very immature and smaller than erythrocytes are situated in the vessel, while another immature islet cell is going to move out from the vessel. Around the vessel, two immature, and several more mature β-cells are developing. In the upper-left corner, an α-cell containing many granules that demonstrated a high electron density is present. The scale bar indicates 2 μm. (b) Transmission electron micrograph (Uranyl acetate-lead citrate stain, ×6,000) of the same graft as shown in figure 2a. A new intercalated duct is surrounded with many new acinar cells, in which a granular endoplasmic reticulum (GER) has developed. Zymogen granules are flowing into the intercalated duct. On the right, a developing acinar cell that does not contain zymogen granules is seen. New acinar cells have proliferated under the old acinar cells. The scale bar indicates 2 μm.
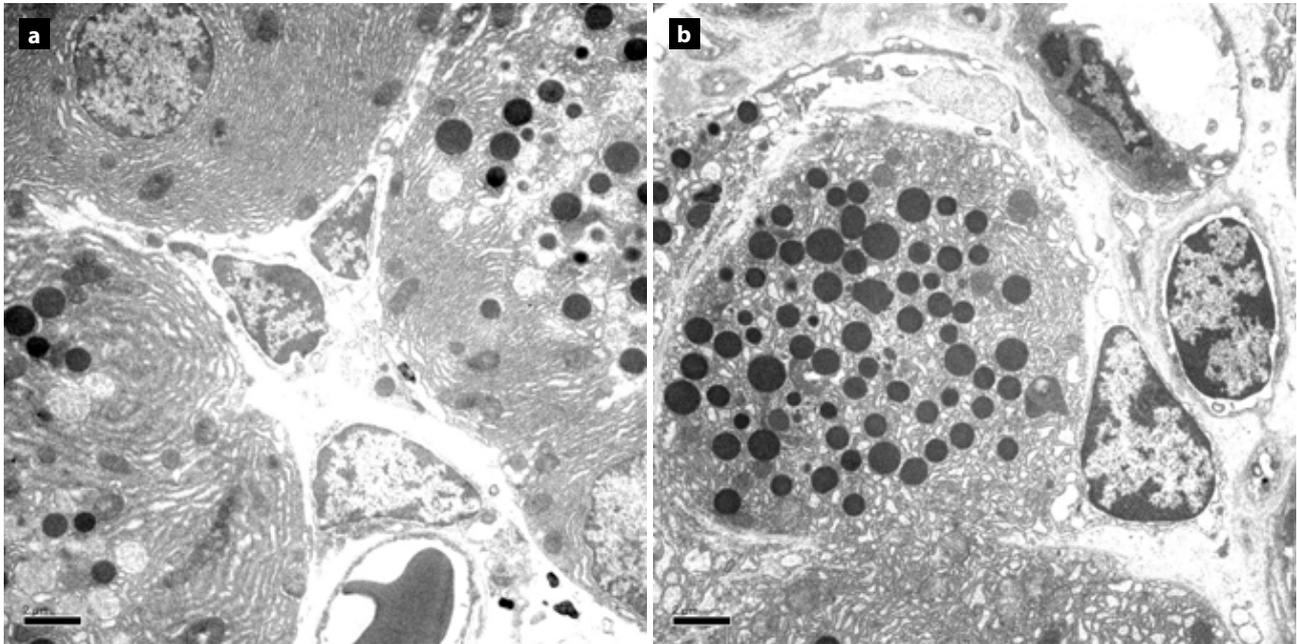
Figure 3. (a) Transmission electron micrograph (Uranyl acetate-lead citrate stain, ×6,000) of the Exp F-5 male graft. The nonparenchymal liner graft showed complete pancreatic regeneration in the Exp F-5 pancreas. Centro-acinar progenitor cells subsequently formed in the center region surrounded by acinar cells. Two of the acinar cells in the upper-left and bottom-right corners contained mitochondria, but did not secrete any zymogen granules. These acinar cells, and especially the bottom-right acinar cell, were immature. All three centro-acinar cells were surrounded with fibrous thin materials, which were the remnants of microcapillary walls. The scale bar indicates 2 μm. (b) Transmission electron micrograph (Uranyl acetate-lead citrate stain, ×6,000) of the graft section from the Exp F-5 male, which also appears in figure 3a. Three centro-acinar progenitor cells are shown on the right side. On the upper-right side, a centro-acinar progenitor cell, that is very immature and smaller than an erythrocyte, is growing normally in a microcapillary and in the microcapillary, another progenitor cell is dying. At the central site, a well-developed centro-acinar cell in a microcapillary is still surrounded by the microcapillary walls. At the bottom site, a centro-acinar progenitor cell is in the process of destroying the microcapillary walls. It is thus demonstrated that a centro-acinar progenitor cell develops in a microcapillary, resulting in the destruction of the microcapillary walls after the centro-acinar progenitor cell has fully developed. The scale bar indicates 2 μm.

light microscopic analysis or TEM analysis.

Table 2 summarizes the FCM results for the host BM, graft BM, and host pancreas. In the BM, Thy-1-positive cells and IGFBP2-positive cells were counted. In the pancreas, IGFBP2-positive cells and insulin-positive cells were counted. A high percentage of BM Thy-1-positive cells tended to be correlated with a high percentage of weakly-positive IGFBP2 BM cells. Due to sexual dimorphism, 3 of the 4 control females (CF) showed high levels (45±3%) of weakly-positive IGFBP2 BM cells, but the 4 control males (CM) showed low levels (5±0.5%) of weakly-positive IGFBP2 BM cells. Figure 4a shows that the Exp F-2 male, which achieved complete pancreatic regeneration, demonstrated a normal level of weakly-positive IGFBP2 BM cells, while the rejected BM graft cells of the Exp E-5 male (BM-graft of Exp E-5) showed a very high level of weakly-positive IGFBP2 BM cells. The Exp C females and Exp F males, of which some rats demonstrated complete pancreatic regeneration after VEGF Ab injection, had normal or suppressed levels of Thy-1-positive and IGFBP2-positive BM cells. Half of the male Exp D rats, however, which were treated with IGF-1R mAb, displayed

moderately high percentages of Thy-1-positive BM cells and high percentages of weakly-positive IGFBP2 BM cells. The Exp D-4 male, which demonstrated complete pancreatic regeneration, showed a moderately high level of Thy-1-positive cells (13%) and a high level of weakly-positive IGFBP2 BM cells (61%). The Exp D-1, 5, and 6 males showed a normal level of weakly-positive IGFBP2 BM cells (6%, 10%, and 7%, respectively), which demonstrated stronger liver graft apoptotic rejection than the Exp D-2, 3, and 4 males that had elevated percentages of weakly-positive IGFBP2 BM cells (44%, 45%, and 61%, respectively). The Exp E males treated with IGF-1R mAb, which did not achieve complete pancreatic regeneration, showed high levels of Thy-1-positive and weakly-positive IGFBP2 BM cells. The Exp E-4, 5, and 6 males, which displayed BM-bone graft necrosis, showed weakly-positive IGFBP2 BM cells of 44%, 28%, and 22%, respectively, while the other 3 rats of the Exp E group, which did not show BM graft necrosis, had a mean weakly-positive IGFBP2 BM cells of 84±5%. Although the weakly-positive IGFBP2 cell percentages were often difficult to measure accurately because of unclear separation from the negative peak, weak IGFBP2 expression was

Table 2. FCM results for the host and graft BM, and host pancreas (fig. 4a).

Exp no (Sex) Total rat	(n)	Sub-rat (n)	BM (Positive cell %)				Pancreas (%)	
			Thy-1	(n)	IGFBP2 (Strong)	(Weak)	IGFBP2	Insulin
Cont (F)	(4)	(1)	15	(1)	1	8	10	—*
		(3)	28±10	(3)	2±2	45±3	64±17	—
A (F)	(4)		18±4		2±0.5	0.6±0.1	59±5	53±9
B (F)	(4)		27±2		3±0.4	9±2	—	—
C (F)	(4)		18±6		3±1	5±2	—	—
Cont (M)	(4)		7±3		1±0.2	5±0.5	—	—
D (M)	(6)	(3)**	15±4	(3)**	2±0.3	50±8	—	—
		(3)†	6±2	(3)†	1±0.5	8±2	—	—
E (M)	(6)		21±6		1±0.5	58±27	—	—
BM-graft	(1)		70 (50)††		4	89	—	—
F (M)	(5)		10±8		0.4±0.1	3±1	—	—

*Not tested, ** D-2, 3, and 4 (rat no), † D-1, 5, and 6, †† Strongly-positive Thy-1%, Cont: Control

clearly affected by not only iGF-1R mAb injection but also immune-regenerative reactions. The Exp B females treated with IGF-1R mAb displayed a normal level of weakly-positive IGFBP2. The immune reactions that occurred in the Exp B females did not lead to the activation of weakly-positive IGFBP2. The frequency of strong BM IGFBP2 expression was only slightly affected by the transplantation, remaining at 0.4% to 3% in all the rats.

The host pancreatic islet cells of the Exp A rats expressed IGFBP2. In the same cell populations, the IGFBP2-positive cell percentage was similar to the insulin-positive cell percentage. It was shown that islet β-cells expressed IGFBP2.

Table 3 shows the FCM results for the host and graft spleen. Spleen cell expression of CD8a, CD25, IGFBP2, and IGF-1R was examined. The CD8a-positive cell percentage of the Exp B females, which showed intra-pancreatic LN enlargement and auto-red blood cell sensitization in the LN, was normal (0.8±0.7). No NK cell activation was observed in the Exp B rats. The CD8a-positive cell percentage was slightly increased to 2.7±0.7% in the Exp E males, which showed BM-bone graft rejection. No changes in the frequencies of CD25- or IL-2R-positive cells were observed in any of all the rats. As shown in figure 4b, the peak for strongly-positive IGFBP2 cells was well separated from the peak for IGFBP2-negative and weakly-positive cells in the spleen. However, the peak for IGF-1R-positive cells was not distinct from the peak for IGF-1R-negative cells. Using the data for the CM-2 rat, the positive threshold for IGF-1R was set so that the threshold was outside of the negative peak. Due to sexual dimorphism, the 4 CF showed high levels

Table 3. Flow cytometry FCM results for the host and graft spleens (sp) (see Fig. 4b).

Exp no (Sex) Group (sex)	Total rat (n)	Spleen (Positive cell %)				
		CD8a	CD25	IGFBP2 (Strong)	(Weak) (n)	IGF-1R
Cont (F)	(4)	0.5±0.1	3±0.2	12±1	50±13	—
A (F)	(4)	0.5±0.2	1±0.1	9±2	16±1	—
B (F)	(4)	0.8±0.7	3±0.2	12±1	14±3	—
Graft-sp	(2)	0.4	2	14	25	—
C (F)	(4)	0.4±0.2	2±0.2	15±2	16±3	—
Cont (M)	(4)	0.4±0.3	2±0.3	13±1	12±2	1±0.5
D (M)	(6)	0.4±0.1	2±0.9	15±2	65±3 (3)*	—
					23±5 (3)**	—
E (M)	(6)	2.7±0.7	3±0.5	17±2	61±7 (4)†	20±6
					35 (2)‡	2
F (M)	(5)	0.2±0.1	2±0.1	12±1	14±1	1±0.3

*D-2, 3, and 4 (rat no), **D-1, 5, and 6, †E-1, 2, 3, and 4 (rat no), ‡E-5 and 6

(50±13%) of weakly-positive IGFBP2 spleen cells, but the 4 CM showed lower levels (12±2%) of weakly-positive IGFBP2 spleen cells. The Exp C-1 and 3 females, the Exp D-4 male, and the Exp F-2, 3, and 5 males, all which had achieved complete pancreatic regeneration, were displayed the following frequencies of strongly-positive IGFBP2 spleen cells (weakly-positive cell %): 12%(14%), 16%(18%), 16%(61%), 12%(14%), 13%(12%), and 14%(15%), respectively. Only the Exp D-4 male, which was injected with IGF-1R mAb, indicated an increased percentage (61%) of weakly-positive

IGFBP2 spleen cells. In the Exp D-4 rat, weakly-positive IGFBP2 cells demonstrated high frequencies in the BM and spleen. Not only BM immature cells, but also spleen lymphocytes frequently expressed weakly-positive IGFBP2 in the Exp D-4 rat. The Exp F males, 60% of which had achieved complete pancreatic regeneration, demonstrated a normal percentage (14±1%) of weakly-positive IGFBP2 spleen cells after VEGF Ab injection. The Exp F males also showed a normal percentage (1±0.3%) of IGF-1R-positive spleen cells, but 4 of the 6 Exp E males that rejected BM-bone grafts after IGF-1R mAb treatment showed elevated numbers (61±7%) of weakly-positive IGFBP2 spleen cells and an increased percentage (20±6%) of IGF-1R-positive spleen cells. Two spleen grafts (Graft-sp of Exp B females) showed normal percentages of CD8a (0.4%), CD25 (2%), and strongly-positive IGFBP2 (14%) cells and a slight increase (25%) in the number of weakly-positive IGFBP2 cells. No increase in weak IGFBP2 expression was induced in their host spleens of the Exp B rats even after IGF-1R mAb injection. The increased frequency of weakly-positive IGFBP2 cells was accompanied by pre-regenerative or regenerative reactions, and rebound activation post-IGF-1R mAb treatment, as found in the Exp D and Exp E males. In all the experimental rats, the strong expression of IGFBP2 in the spleen was barely affected by immune reactions, as found in the BM, maintaining levels of 9±2% to17±2%.

Figure 5a shows the electron micrograph of a BM segmented neutrophil that has been immunochemically stained with IGFBP2 Ab-gold in the Exp D-2. The round site showing a markedly high electron density represents extracellular IGFBP2 bound to IGFBP2 Ab-gold particles. The strongly-positive IGFBP2 cells were demonstrated to be the cells showing extracellular IGFBP2 on their surface membrane. Many gold particles bound to the IGFBP2-IGFBP2 Ab complexes. Many segmented neutrophils displayed extracellular IGFBP2 in the BM, although neutrophil
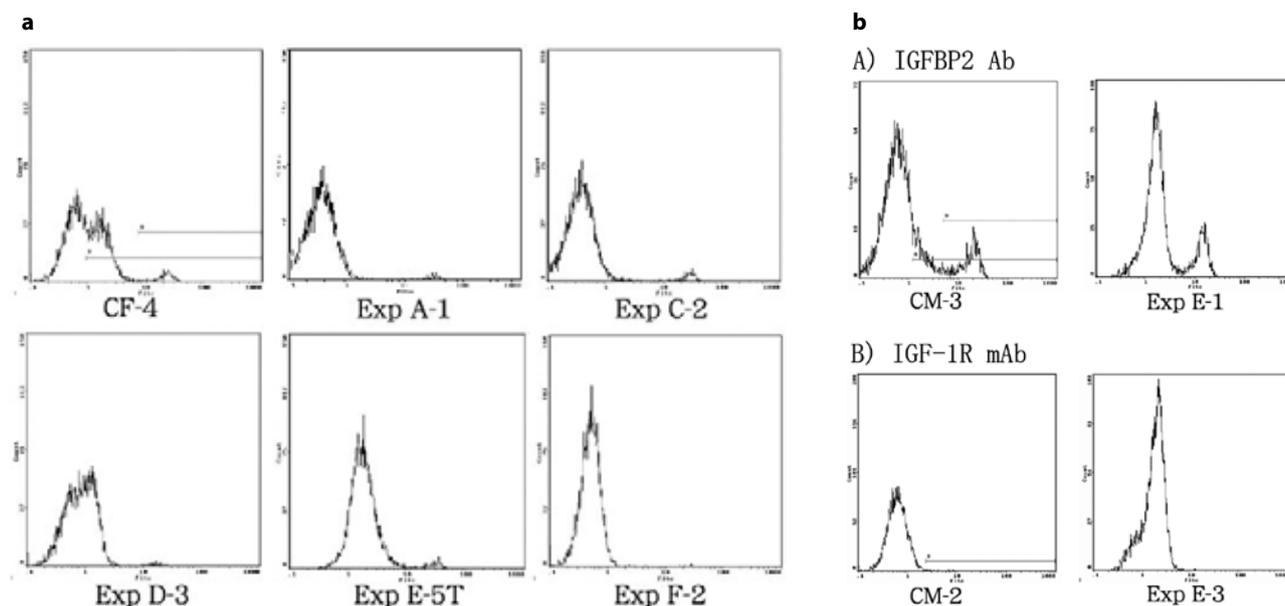

Figure 4. (a) FCM results for the BM MNC stained with FITC-IGFBP2 Ab. The long side line for CF-4 indicates the total frequency of the weakly (w)- and strongly (s)-positive IGFBP2 BM cells, and the short side line only indicates the percentage of strongly-positive IGFBP2 BM cells. Sexual dimorphism was detected in IGFBP2 expression. The results for females are shown at the top of this figure and the results of males are shown at the bottom of this figure. The Exp C-2 and Exp F-2 rats were injected with VEGF Ab, and the Exp D-3 and Exp E-5 rats were injected with IGF-1R mAb. The Exp A-1 rat was not injected with any Ab. Compared with the CM BM, which contained 4.9±0.5% of weakly-positive IGFBP2 (tab. 2), the Exp D-3 male BM and the BM grafts of the Exp E-5 male showed increased numbers of weakly-positive IGFBP2 cells. The Exp A-1 female and the Exp C-2 female demonstrated reduced numbers of weakly-positive IGFBP2 cells, compared with those of the CF-2. The Exp F-2 male, which achieved complete pancreatic regeneration, demonstrated a normal level of weakly-positive IGFBP2 cells. Among them, the frequencies of strongly-positive IGFBP2 cells changed little in the BM. The percentages of IGFBP2-positive BM cells were as follows: CF-4: 44% (w) and 4% (s), Exp A-1: 1% (w) and 2% (s), Exp C-2: 4% (w) and 4% (s), Exp D-3: 45% (w) and 1% (s), BM grafts of Exp E-5 (Exp-5T): 89% (w) and 4% (s), and Exp F-2: 5% (w) and 0.4% (s). (b) FCM results for MNC stained with FITC-IGFBP2 Ab and FITC-IGF-1R mAb. All the results were obtained from males. The IGFBP2 results are shown on the top, and the IGF-1R results are shown on the bottom. The long side line for CM-3 indicates the total frequencies of weakly (w)-positive and strongly (s)-positive cells, and the short line only indicates the frequency of the strongly-positive cells. The IGFBP2-positive cell frequencies of the spleen MNCs were as follows: CM-3: 13% (w) and 13% (s), and Exp E-1: 61% (w) and 19% (s). Although the percentage of strongly-positive IGFBP2 cells did not differ much between the CM-4 and Exp E-1 rats, the percentage of weakly-positive IGFBP2 cells differed much between them. On the bottom, the long side line for CM-2 indicates the overall frequency of weakly (w)- and strongly (s)-positive cells. The IGF-1R-positive cell frequencies of the spleen MNCs were as follows: CM-2: 0.7%, and Exp E-3: 27%. In the Exp E rats that were injected with IGF-1R mAb, the spleen MNCs demonstrated elevated levels of not only weakly-positive IGFBP2 but also weakly-positive IGF-1R.

IGFBP2 was not counted in the FCM. Figure 5b shows an electron micrograph stained immunochemically. A BM premature lymphocyte obtained from the Exp D-2 BM had the IGFBP2 site stained with IGFBP2-gold particles. Figure 6a shows an immunochemically stained electron micrograph of spleen lymphocytes found in the Exp D-2 rat. Of the two lymphocytes, one was a strongly-positive IGFBP2 cell, which was detected at a high density site. The other was a weakly-positive IGFBP2 cell, the mitochondrial membranes of which expressed intracellular IGFBP2. The spleen of the Exp D-2 male had a weakly-positive IGFBP2 cell frequency of 70% and a strongly-positive IGFBP2 cell frequency of 13% in the FCM. Although complete pancreatic regeneration was not achieved in the Exp D-2 rat, weak IGFBP2 activation occurred in this male. Figure 6b shows a spleen lymphocyte stained positively with IGF-1R mAb-gold particles, detected in the Exp E-1 male after IGF-1R mAb injection. The smaller density site than that of IGFBP2 stained with IGF-1R mAb-gold particles represents extracellular IGF-1R, in which the frequency of IGF-1R-positive cells was 25%. The Exp E-1 male spleen demonstrated elevated levels of a weakly-positive IGFBP2 cell frequency of 61% and a strongly-positive IGFBP2 cell frequency of 19%. It was shown that activated IGF-1R was correlated with activated IGFBP2. Soluble large IGFBP2 particles bound to IGFBP2 Ab-gold were observed, some of which were in contact with the surface membranes of erythroid precursors. In the spleens of the Exp D-2 and Exp E-1 rats, IGFBP2-positive monocytes were also detected.

Figure 7a shows a host pancreatic β-cell detected in the Exp D-5 male. It was immunochemically stained with IGFBP2 Ab-gold particles. The β-cell contained a large granule that was stained with IGFBP2 Ab-gold, which was not an insulin secretory granule. The large IGFBP2-positive granule had a very thick outer membrane and an interior space. It was judged originally to be the same extracellular IGFBP2 as found in neutrophils, BM premature lymphocytes, and spleen lymphocytes. Figure 7b is an electron micrograph of an immunochemically stained host pancreatic β-cell found in the Exp D-1 male. The β-cell was more immature than that of figure 7a. Its IGFBP2-positive granule of high electron density was smaller than that shown in figure 7a, but the characteristics of the IGFBP2-positive granule were identical to the IGFBP2 granule shown in figure 7a. IGFBP2 must be induced during the development of premature islet cells together with other secretory granules. These results obtained from the electron micrographs did not contradict the pancreatic FCM results reported above.
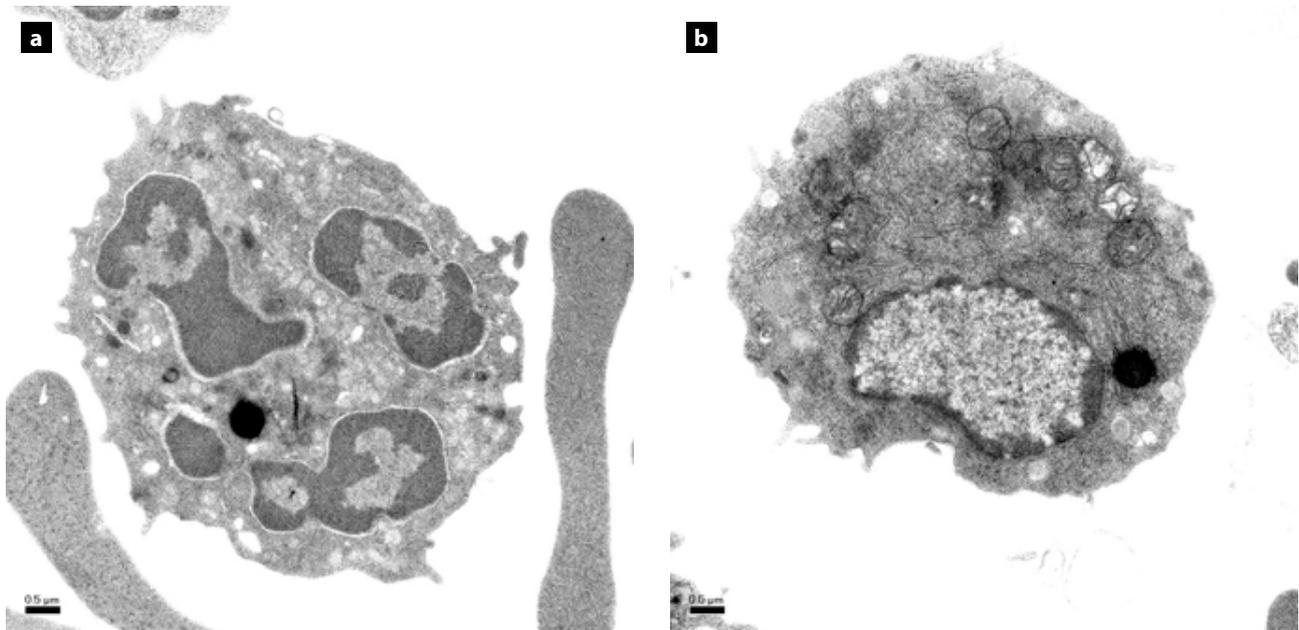
Figure 5. (a) Transmission electron micrograph (Uranyl acetate-lead citrate stain, ×15,000) showing a host BM cell from the Exp D-2 rat, in which its BM cells were stained with IGFBP2 Ab-gold complexes before fixing. The rat was injected with anti IGF-1R mAb. The IGFBP2-positive segmented neutrophil presented here was detected in the BM. Extracellular IGFBP2 was positively stained with IGFBP2 Ab-gold complexes, producing a round site with a high electron density. Many neutrophils, which were not counted in the BM FCM, expressed the same extracellular IGFBP2 as shown here. The scale bar indicates 0.5 μm. (b) Transmission electron micrograph (Uranyl acetate-lead citrate stain, ×15,000) of the same BM stained with IGFBP2 Ab-gold complexes before fixing as shown in figure 5a. The prolymorphocyte containing many mitochondria displays the same IGFBP2-positive site of a high electron density as is shown in figure 5a. The lymphocyte was counted as a strongly-positive IGFBP2 mononuclear cell (MNC) on the BM flow cytometry (FCM). The scale bar indicates 0.5 μm.
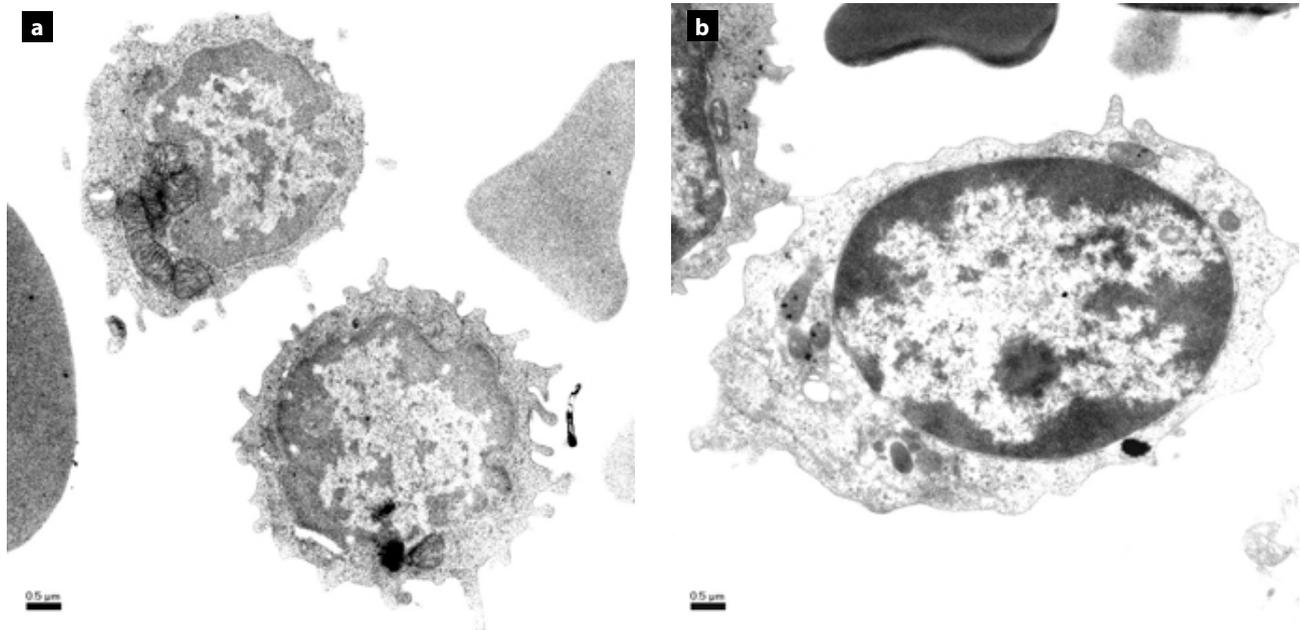
Figure 6. (a) Transmission electron micrograph (Uranyl acetate-lead citrate stain, ×15,000) showing spleen cells from the Exp D-2 rat treated with IGF-1R mAb, which were stained with IGFBP2 Ab-gold complexes before fixing. Two spleen lymphocytes that were positively stained with IGFBP2 Ab-gold complexes are seen. The mitochondrial membranes of the top spleen lymphocyte were positively stained with IGFBP2 Ab-gold, which was shown as weakly-positive IGFBP2 in the FCM. The bottom spleen lymphocyte displays extracellular IGFBP2 stained with IGFBP2 Ab-gold complexes, which was shown as strongly-positive IGFBP2 in the FCM. The scale bar indicates 0.5 μm. (b) Transmission electron micrograph (Uranyl acetate-lead citrate stain, ×15,000) showing a spleen cell from the Exp E-1 rat treated with IGF-1R mAb. Before fixing, the spleen cells were stained with IGF-1R mAb-gold complexes. The spleen lymphocyte shown here is positively stained with IGF-1R mAb-gold complexes. The IGF-1R site shows a very high electron density. This rat demonstrated elevated IGF-1R activity on the flow cytometry (FCM). The scale bar indicates 0.5 μm.
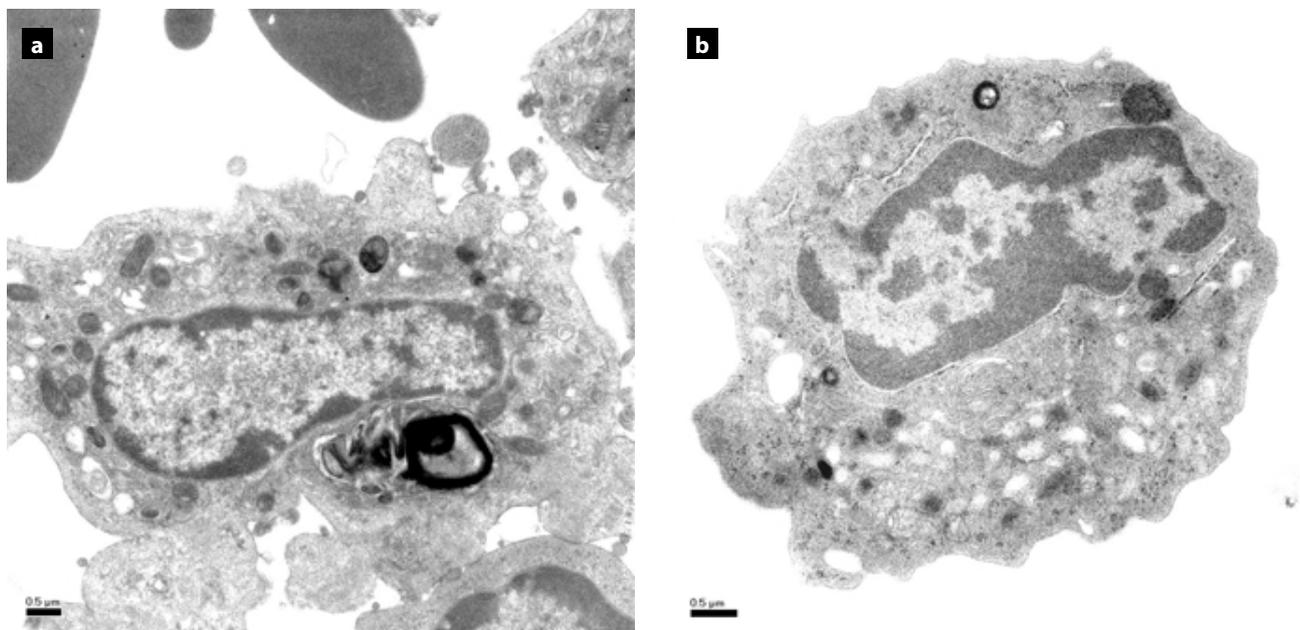

Figure 7. (a) Transmission electron micrograph (Uranyl acetate-lead citrate stain, ×15,000) showing a host pancreatic cell from the Exp D-5 rat treated with IGF-1R mAb. Before fixing, the pancreatic cells were stained with IGFBP2 Ab-gold complexes. An islet β-cell that has been positively stained with IGFBP2 Ab-gold complexes is shown. The IGFBP2 site, which demonstrates a high electron density, has a similar structure to the large secretory granule observed in the β-cell. Basically, the IGFBP2 site is the same as the extracellular IGFBP2 found in the hematopoietic cells mentioned above. The scale bar indicates 0.5 μm. (b) Transmission electron micrograph (Uranyl acetate-lead citrate stain, ×20,000) showing a host pancreatic cell from the Exp D-1 male, which belonged to the same group as the rat shown in figure 7a. Before fixing, the pancreatic cells were also stained with IGFBP2 Ab-gold complexes. The islet β-cell shown here is more immature than that shown in figure 7a. An IGFBP2-positive site is present at the top of the cytoplasm, which is smaller than that shown in figure 7a. However, the IGFBP2 structure is the same as that shown in figure 7a. The scale bar indicates 0.5 μm.

DISCUSSION

In this study, complete pancreatic regeneration, including the islets of Langerhans, acinar cells, and duct cells, was developed from the nonparenchymal liver and BM clot grafts. As the possible original cells of complete pancreatic regeneration, very small embryonic-like stem cells (VSEL) were speculated, mainly because pancreatic progenitor cells smaller than erythrocytes were detected in this study. VSEL cells have diameters of 3.63±0.14 μm and 6.58±1.09 μm in mice and humans, respectively, are larger than peripheral blood platelets but smaller than erythrocytes and have been identified as non-hematopoietic BM cells that possess regenerative capacity.[5] The BM is the main organ harboring VSEL, but the pancreas and fetal liver also contain VSEL. Although the hematopoietic stem cells (HSC) or resident VSEL in the pancreas have the plasticity to regenerate pancreatic cells, and especially β-cells, it is difficult for the regenerated cells to move out from the blood vessels. Islet β-cells were regenerated from HSC, and observed to proliferate in blood vessels without forming normal islets of Langerhans, as was also found in the host with the BM-bone graft necrosis.[6] Resident VSEL in the pancreas demonstrated limited pancreatic β-cell expansion in the rats with partial pancreatic resection, BM VSEL must have more pluripotent capability for pancreatic generation than resident VSEL. For active regeneration, it was very important that all the three kinds of pancreatic progenitor cells had the ability to move out from blood vessels, and destroy the vessel walls, as sooner or later, any regenerated cells remaining in the vessels would become apoptotic. In this study, concerning the regeneration of islets of Langerhans, islet progenitor cells smaller than erythrocytes regenerated in the blood vessels as a consequence of VSEL migration from the host BM to pancreatic graft vessels. The regenerated small islet cells moved out from the vessels and matured outside them under suspicion of vessel apoptosis. Regarding the regeneration of centro-acinar cells, it was shown that centro-acinar progenitor cells smaller than erythrocytes were regenerated in microcapillaries as a consequence of VSEL migration into the microcapillaries. After a centro-acinar progenitor cell developed in a microcapillary, it destroyed the microcapillary walls. Regarding acinar cells, it was suspected that the first new acinar cell was generated from migrating VSEL, resulting in mature cell mitosis on the outside of the vessels. All these findings with regard to complete pancreatic regeneration could be explained with reference to the results obtained from the liver and BM clot grafts. As the regenerative patterns were identical in both the liver and BM clot grafts, it was concluded further strongly that the epiblast/germ line-derived VSEL had migrated from the host BM to the injured and ischemic nonparenchymal liver graft or BM clot graft. The grafted microenviromental cells that surrounded the blood vessels were very important for complete pancreatic regeneration.

Physiologically, pancreatic progenitors develop into acinar cells, pancreatic ductal cells and endocrine progenitors in the presence of different regulatory factors.[2] It was shown that duct cell development lagged behind that of acinar cells. After acinar cells had been regenerated, centro-acinar cells developed in microcapillaries. During early embryonic development, hepatocyte nuclear factor-6 (HNF-6)/Onecut-1 (OC-1) is expressed in the buds, and at mid-gestation, HNF-6 is expressed in the proto-differentiated epithelium.[7] HNF-6 acts upstream of Pdx-1 in the specification cascade. In late gestation, HNF-6 is downregulated in pancreatic endocrine cells. The acinar cells that did not express the Hnf6 gene were mobilized first, and then the duct cells that were regulated by the Hnf6 gene were specifically mobilized to the regions where acinar cells had regenerated first. Compared with the liver grafts, the BM clot grafts showed more active regeneration of duct cells. In the BM, the Hnf6 gene must function more actively than in the liver. It was also speculated that the BM contained more immature VSEL than persistent pancreatic VSEL.

The IGF system includes two peptide hormones IGF-1 and -2, the receptors IGF-1R and -2R, six soluble IGFBP (1−6), and IGFBP protease.[8] IGF-1 and -2 are small signaling proteins mediated by IGF-1R. BM mesenchymal stem cells (MSC), which are surrounded by hematopoietic microenviromental cells including vascular smooth muscle-like stromal cells, adipocytes, osteoblasts, and endothelial cells, can produce IGF-1, and the autocrine interaction of IGF-1 with IGF-1R induces their pro-migratory, proliferation, and differentiation activities in MSC expressing a moderate level of IGF-1R.[9] Growth hormone (GH) and IGF-1 stimulate the expansion of primitive multilineage CD34+CD38- hematopoietic progenitor cells and increase the yields of several hematopoietic subpopulations.[10] The IGF-1/IGF-1R system activation is very important in BM MSC for mobilizing immature VSEL from the host BM. The subsequent activation of matrix metalloproteinase (MMP) is also necessary for mobilizing MSC. It was shown that MMP1 is critically involved in the migration capacity of human BM MSC towards human glioma through the MMP1/protease-activated receptor 1 (PAR1) axis.[11] The MSC of the BM clot graft and the nonparenchymal cells of the liver graft, which express the GF-1/IGF-1R system, must be also involved in accepting mobilized BM VSEL prior to pancreatic regeneration. IGF-1 is mainly synthesized

in hepatocytes, but IGF-1R is predominantly expressed in hepatic stellate cells and Kupffer/endothelial cells, which demonstrate significantly reduced expression of IGF-1 in nonparenchymal liver graft.[12] In this study, high levels of nonparenchymal liver graft IGF-1R correlated well with the best pancreatic regeneration results. In the whole liver transplantation group, complete pancreatic regeneration was achieved in one of the 6 rats when anti-IGF-1R mAb was injected into the host spleen. In the rats that received a whole liver graft, rebound activation of IGF-1R due to IGF-1R mAb injection triggered complete pancreatic regeneration. IGF-1R and IGFBP2 activation due to IGF-1R mAb injection were demonstrated well by elevated frequencies of weak IGFBP2 and weak IGF-1R expression in FCM analyses. A previous report also described similar rebound activation at post-Ab injection.[13]

IGFBP binds strongly to IGF. Proteolysis enables IGF to bind to and activate the cell surface IGFR after proteolysis has dissolved the binding. IGFBP2, which was analyzed in this study, exists as a monomer and exhibits a unique intra-molecular disulfide-bonding pattern.[8] IGFBP2 overexpression has been detected in colorectal, adrenal, ovarian, prostate, lung, and breast cancers; glioma; and leukemia. Membrane-associated IGFBP2 stimulates cell proliferation and migration through direct binding to serum and extracellular matrix molecules, such as integrin receptors, proteoglycans, and heparin. Intracellular IGFBP2 overexpression in lung adenocarcinoma has been shown to induce a substantial decrease in procaspase-3 expression and thereby protect cells against apoptotic reactions in an IGF-independent manner.[14] In this study, membrane-associated IGFBP2 and intracellular IGFBP2 expressed on the mitochondrial membranes of hematopoietic cells were detected in FCM and TEM analyses. Compared with the reversible and sexually dimorphic nature of intracellular IGFBP2 expression, membrane-associated IGFBP2 expression is more tightly regulated at the genetic level. Biochemical analyses have uncovered both zebrafish igfbp-2a and -2b genes. In adult males, IGFBP-2b mRNA is only detected in the liver, but in adult females, IGFBP-2b mRNA is detected in the liver,

gut, kidney, ovary, and muscle.[15] The observed sexual dimorphism was partly explained by differences in mRNA expression between the sexes. The islet β-cells expressed membrane-associated IGFBP2, but not the acinar cells. Increased levels of serum IGFBP2 are found in DM, and the IGFBP2 protein and mRNA levels in lung cancer cells are dependent on glucose concentration.[14] The IGFBP gene is one of the genes responsible for diabetic nephropathy.[16] A close relationship between IGFBP2 and DM has been demonstrated, which implies that β-cell IGFBP2 expression is involved in DM. In this study, β-cell IGFBP2 expression was shown to be the same as these of hematopoietic cells. HSC had the same origin as β-cell.

VEGF is an important mediator of angiogenesis, which is antagonistic to complete pancreatic regeneration. Anti-VEGF Ab injection into the host spleen, which was used in this study, produced good results. The overexpression of IGF-1R and IGFBP2 does not lead to VEGF activation, the mechanisms of which can be explained as follows:[17] IGR-1R and IGFBP2 upregulate the phosphatidyl inositol 3 kinase (PI3K) and phosphatase and tensin homolog deleted on chromosome ten (PTEN) pathways. PTEN cleavage is downregulated by the decreased procaspase-3 level, which is brought about by IGF-1R/IGFBP2 overexpression. The upregulation of PTEN suppresses VEGF activation. The transcription factor specific protein 1 (Sp1) is required for the transactivation of VEGF. However, judging from the decreased level of procaspase-3, Sp1 must be inhibited by IGF-1R/IGFBP2 activation. It can be said that VEGF activation is inhibited by IGF-1R/IGFBP2 activation.

Therefore, rebound IGF-1R activation, which was induced by IGF-1R mAb injection, theoretically reacted as like as anti-VEGF injection. However, as shown in these experimental results, it was concluded that VEGF Ab was more useful for pancreatic regeneration than IGF-1R mAb, which induced rebound activation of intracellular IGF-1R and IGFBP2. After pancreatic regeneration, increased levels of soluble IGFBP2 would disturb the regenerated islet β-cells. Duct cell regeneration must be suppressed by IGF-1R/IGFBP2 overexpression, as was found in a whole liver graft.

ΠΕΡΙΛΗΨΗ

Πλήρης αναγέννηση του παγκρέατος, περιλαμβανομένων των νησιδίων του Langerhans, των κυττάρων των αδενοκυψελών, των κυττάρων του κέντρου των κυψελών, των διάμεσων και των εκκριτικών κυττάρων των πόρων σε ποντίκια Lewis

T. NAKATSUJI

Department of Transfusion Cell Therapy, Hamamatsu University, School of Medicine, Hamamatsu, Ιαπωνία

Αρχεία Ελληνικής Ιατρικής 2011, 28(1):89–102

ΣΚΟΠΟΣ *In vivo* επεξήγηση συστημάτων για την πλήρη αναγέννηση του παγκρέατος σε μοντέλα ζώων. **ΥΛΙΚΟ-ΜΕΘΟΔΟΣ** Με τη χρήση μόνο ομοιογονιδιακών ποντικών Lewis έγινε μεταμόσχευση ήπατος, μυελού των οστών με οστό, πήγματος μυελού των οστών ή μη παρεγχυματικών ηπατικών κυττάρων στο πάγκρεας του ξενιστή. Επί πλέον, έγινε έγχυση στο σπλήνα του ξενιστή είτε μονοκλωνικού αντισώματος IGF-1R είτε αντισώματος VEGF. Τα πειραματόζωα παρακολουθήθηκαν για 5,5–6 μήνες. Μετρήθηκε η IGFBP2 σε αιμοποιητικά μονοπύρηνα κύτταρα και σε κύτταρα του παγκρέατος με κυτταρομετρία ροής. Επίσης, εφαρμόστηκαν αναλύσεις με ηλεκτρονικό μικροσκόπιο για τις εμβρυολογικές μελέτες του αναγεννώμενου παγκρέατος. **ΑΠΟΤΕΛΕΣΜΑΤΑ** Η πλήρης αναγέννηση του παγκρέατος, περιλαμβανομένων αφ' ενός των ενδοκρινών και αφ' ετέρου των εξωκρινών κυττάρων, επιβεβαιώθηκε σε 2 (50%) από τα 4 θηλυκά ποντίκια που έλαβαν μοσχεύματα πήγματος μυελού των οστών και αντίσωμα VEGF, σε 1 (17%) από τα 6 άρρενα ποντίκια που έλαβαν μοσχεύματα πλήρους ήπατος και μονοκλωνικό αντίσωμα IGF-1R, καθώς και σε 3 (60%) από τα 5 άρρενα ποντίκια που έλαβαν μη παρεγχυματικά ηπατικά μοσχεύματα και αντίσωμα VEGF. Στην κυτταρομετρία ροής, αυξήθηκαν τα ασθενώς θετικά IGFBP2 κύτταρα λόγω της παλίνδρομης ενεργοποίησης από την έγχυση του μονοκλωνικού αντισώματος IGF-1R. Επίσης, στα β-κύτταρα των νησιδίων εκφράστηκε η IGFBP2. Μικρότερα νησιδιακά κύτταρα σε σχέση με τα ερυθροκύτταρα αναγεννήθηκαν στα αγγεία και αναπτύχθηκαν και εξωαγγειακά. Ένα μικρότερο κύτταρο του κέντρου των κυψελών σε σχέση με ένα ερυθρό αναγεννήθηκε σε ένα τριχοειδές, τα τοιχώματα του οποίου καταστράφηκαν μετά από την πλήρη ανάπτυξη. Τα κύτταρα των κυψελών πολλαπλασιάστηκαν με μίτωση, όπως τα φυσιολογικά εκτός των αιμοφόρων αγγείων. **ΣΥΜΠΕΡΑΣΜΑΤΑ** Τα μοσχεύματα των μη παρεγχυματικών ηπατικών κυττάρων και των πηγμάτων μυελού των οστών έχουν όμοιο αποτέλεσμα στην αναγέννηση του παγκρέατος. Αρχέγονα κύτταρα από το μυελό των οστών του ξενιστή μετακινούνται στα μοσχεύματα, με αποτέλεσμα την πλήρη αναγέννηση του παγκρέατος.

Λέξεις ευρετηρίου: IGFBP2, IGF-1R, Μη παρεγχυματικά ηπατικά μοσχεύματα, Πλήρης παγκρεατική αναγέννηση, VEGF

References

1. NOGUCHI H, OISHI K, UEDA M, YUKAWA H, HAYASHI S, KOBAYASHI N ET AL. Establishment of mouse pancreatic stem cell line. *Cell Transplant* 2009, 18:563–571
2. ZARET KS, GROMPE M. Generation and regeneration of cells of the liver and pancreas. *Science* 2008, 322:1490–1494
3. SLACK JMW. Metaplasia and transdifferentiation: From pure biology to the clinic. *Mol Cell Biol* 2007, 8:369–378
4. DE-MIGUEL MP, ARNALICH-MONTIEL F, LOPEZ-IGLESIAS P, BLAZQUEZ-MARTINEZ A, NISTAL M. Epiblast-derived stem cells in embryonic and adult tissues. *Int J Dev Biol* 2009, 53:1529–1540
5. ZUBA-SURMA EK, KUCIA M, RATAJCZAK J, RATAJCZAK MZ. "Small stem cells" in adult tissues: Very small embryonic-like stem cells (VSELs) stand up! *Cytometry A* 2009, 75:4–13
6. NAKATSUJI T. Bone marrow (BM) stem cells developed into pancreatic β cells and acinar cells in the Lewis rats having more than 30% of γδ T cell receptor (TCR)-positive lymphocytes. *Haema* 2006, 9:61–70
7. JACQUEMIN P, LEMAIGRE FP, ROUSSEAU GG. The Onecut transcription factor HNF-6 (OC-1) is required for timely specification of the pancreas and acts upstream of Pdx-1 in the specification cascade. *Dev Biol* 2003, 258:105–116
8. SWAIN M, SLOMIANY MG, ROSENZWEIG SA, ATREYA HS. High-yield bacterial expression and structural characterization of recombinant human insulin-like growth factor binding protein-2. *Arch Biochem Biophys* 2010, 501:195–200
9. PONTE AL, MARAIS E, GALLAY N, LANGONNÉ A, DELORME B, HÉRAULT O ET AL. The *in vitro* migration capacity of human bone marrow mesenchymal stem cells: Comparison of chemokine and growth factor chemotactic activities. *Stem Cells* 2007, 25:1737–1745
10. HANLEY MB, NAPOLITANO LA, McCUNE JM. Growth hormone-induced stimulation of multilineage human hematopoiesis. *Stem Cells* 2005, 23:1170–1179
11. HO IAW, CHAN KYW, NG W-H, GUO CM, HUI KM, CHEANG P ET AL. Matrix metalloproteinase 1 is necessary for the migration of human bone marrow-derived mesenchymal stem cells toward

human glioma. *Stem Cells* 2009, 27:1366–1375

12. SOBREVALS L, RODRIGUEZ C, ROMERO-TREVEJO JL, GONDI G, MON-REAL I, PAÑEDA A ET AL. Insulin-like growth factor I gene transfer to cirrhotic liver induces fibrolysis and reduces fibrogenesis leading to cirrhosis reversion in rats. *Hepatology* 2010, 51:912–921

13. NAKATSUJI T. Immune tolerance induced by the inhibition of CD18 alone or both signal transducer and activator of transcription 3 (Stat3) and islet/duodenum homeobox-1 (IDX-1) at the time of rat bone marrow (BM) transplantation in which thymus T lymphopoiesis occurred post-transplantation. *Arch Hellen Med* 2010, 27:529–538

14. ZHOU J, LI W, KAMEI H, DUAN C. Duplication of the IGFBP-2 gene in teleost fish: Protein structure and functionality conservation and gene expression divergence. *PLoS ONE* 2008, 3:e3926

15. MIGITA T, NARITA T, ASAKA R, MIYAGI E, NAGANO H, NOMURA K ET AL. Role of insulin-like growth factor binding protein 2 in lung adenocarcinoma: IGF-independent antiapoptotic effect via caspase-3. *Am J Pathol* 2010, 176:1756–1766

16. GUTTULA SV, RAO AA, SRIDHAR GR, CHAKRAVARTHY MS, NAGESHWARARO K, RAO PV. Cluster analysis and phylogenetic relationship in biomarker identification of type 2 diabetes and nephropathy. *Int J Diabetes Dev Ctries* 2010, 30:52–56

17. PORE N, LIU S, SHU H-K, LI B, HAAS-KOGAN D, STOKOE D ET AL. Sp1 is involved in Akt-mediated induction of VEGF expression through an HIF-1-independent mechanism. *Mol Biol Cell* 2004, 15:4841–4853

Corresponding author:

T. Nakatsuji, Department of Transfusion Cell Therapy, Hamamatsu University, School of Medicine, 1-20-1 Handayama, Higashi-ku, Hamamatsu 431-3192, Japan
e-mail: nh80415@hama-med.ac.jp